ISSN 2616-5880 Vol. 5, Issue 2: 46-54, DOI: 10.25236/AJMC.2024.050208

Purification of swine wastewater using a biological aerated filter with non-sintered foundry dust based ceramsite

Yue Zhang

School of Environmental Science and Engineering, Nanjing University of Information Science & Technology (NUIST), Nanjing, Jiangsu, China
827504959@qq.com

Abstract: *The non-sintered foundry dust (FD) based ceramsite formed by curing steam (FDNCCS), and non-sintered FD based ceramsite formed by curing CO_2 (FDNCCC) were obtained under steam temperature of 80℃ for 16 h, and air humidity at 70%, temperature at 20°C, and CO_2 volume fraction of 20% for 2 h. The compressive strength, specific surface area, and the water absorption rate were respectively 5.18 MPa, 48.1%, and 22.4% for FDNCCC. Compressive strengths of FDNCCC were found to be 2.2 times than that of FDNCCS. The specific surface areas of and total pore volumes of commercial non-sintered ceramsite (CNC), FDNCCS, and FDNCCC were respectively 12.04 m^2/g and 0.0621 cm^3/g, 27.46 m^2/g and 0.0795 cm^3/g, and 28.11 m^2/g and 0.1328 cm^3/g, indicating that FDNCCC and FDNCCS have higher the specific surface area than that of CNC, and the total pore volume of FDNCCC is nearly twice that of the other two types of ceramsites. Biofilm was easy to form on the surface of FDNCCC as biocarrier in biological aerated filters (BAF), and the removal rate of COD, NH_4^+-N, TN, and phosphate were respectively 75%-85%, 80%-90%, 55%-65%, and >85% were obtained when BAF with FDNCCC as biocarrier was used to treat swine wastewater.*

Keywords: *Foundry dust; Non-sintered ceramsite; Swine wastewater; Carbonation curing*

1. Introduction

Production of swine wastewater has gradually increased with the continuous development of the livestock and poultry farming industry in China, resulting in it becoming China's main source of agricultural non-point source pollution[1]. The high concentrations of pollutants in swine wastewater, such as organic matter, nitrogen, phosphorus, suspended solids, and a large number of pathogenic microorganisms, can lead to changes in the ecological environment, and pose a threat to animal and human health[2]. Therefore, it is desirable to treat swine wastewater to reduce risk to the environment and health.

Biological aerated filter (BAF) is a treatment technology commonly used to remove pollutants. BAF has many advantages, such as small footprint, high efficiency, and low cost, and has therefore been widely used to purify wastewaters, including urban and industrial wastewater [3], eutrophic rivers [4], and domestic wastewater[5]. Liu et al.[6] for example, found that following treatment with BAF the quality of effluent met the required discharge standard. However, Xin et al. [7] indicated that performance could be further improved by using a biochar rather than ordinary filter media because this provided a more stable environment for functional bacteria resulting in significantly improved removal performance of total nitrogen (TN) and total phosphorus (TP) from swine wastewater. These findings suggest that development of novel biocarriers for BAF will be important to improve the purifying capacity.

Ceramsite has been used as a biocarrier for BAF because of its properties including a rough surface, large surface area, strong biocompatibility, fast biofilm formation, and uniform particle size distribution. In addition, ceramsite has a chemical stability, allowing it to adapt to treat different wastewater. Ceramsite can be prepared by sintering under high temperature and by non-sintering at room temperature, the latter using less energy and costing less [8]. In addition, the non-sintered ceramsite usually has lower density than that of sintered ceramsite, which also improves efficiency of treatment wastewater.

Curing is an important process for preparing non-sintered ceremsite and can be achieved through different methods including natural curing, steam curing, and steam pressure curing. Natural curing is usually carried out at around 25 ℃, but requires a long curing time, typically 20-90 d[8]. Steam curing

ISSN 2616-5880 Vol. 5, Issue 2: 46-54, DOI: 10.25236/AJMC.2024.050208

can significantly increase the strength of the ceramsite in a shorter period of time due to the diffusion of water vapor, and hydration reactions within the ceramsite. The temperature and duration time for steam curing is generally between 50-100℃and 8-48 h [9], indicating that steam curing process happens under relatively higher temperature. Steam pressure curing is a process under high temperature and high pressure conditions, and therefore is energy intensive. Therefore, each curing method has disadvantages such as the longer curing time, the relatively higher temperature, and the cost of higher energy consumption. Therefore, it is very important to develop better curing methods to prepare ceramites.

CO_2 curing is an alternative and innovative method whereby the hydration products of cement and the cement clinker itself react with CO_2 to produce substances such as carbonates to enhance the concrete strength [10]. The process firstly involves the dissolution of CO_2 gas in the water present in the pores of the concrete to form carbonic acid. The second step involves the carbonation reaction between carbonic acid and the alkaline components in the gel materials and aggregates, such as calcium silicate (C_2S), tricalcium silicate (C_3S), hydrated product $Ca(OH)_2$, and C-S-H gel, to form $CaCO_3$, resulting in achieving permanent storage of CO_2 and improving the concrete strength [11]. The CO_2 curing method has advantages, such as the shorter curing time, lower energy consumption, the higher strength, and fixation of CO_2. However, there is little information on the application of CO_2 curing to prepare non-sintered ceramsite.

2. Materials and methods

2.1 Materials

The FD and fly ash (FA) were obtained from an environmental protection technology company in Ma'anshan City, Anhui Province, in China. The main chemical composition and content are shown in Table 1.

Table 1: *Main chemical composition and content of foundry dust and fly ash (%).*

Chemical Composition	SiO_2	Al_2O_3	CaO	Fe_2O_3	MgO	Na_2O	K_2O	TiO_2
Foundry dust	69.09	14.24	2.57	5.93	2.1	2.4	1.86	/
Fly ash	32.56	37.07	9.404	8.285	1.354	2.767	1.28	1.956

The swine wastewater was obtained from a breeding farm in Luhe District, Nanjing City, in China. The chemical oxygen demand (COD), ammonia nitrogen (NH_4^+-N), total nitrogen (TN), and phosphate concentrations for swine wastewater was 373.33 - 506.67 mg/L, 88.09 -112.59 mg/L, 106.73 - 131.23 mg/L, and 27.19 - 32.22 mg/L, respectively.

The simulated swine wastewater was prepared using chemical reagents, such as anhydrous glucose, ammonium chloride, potassium dihydrogen phosphate, calcium chloride, anhydrous magnesium sulfate, and hexahydrate ferric chloride. The concentration of f COD, ammonia nitrogen, and phosphate present in the simulated swine wastewater were 1200 mg/L, 150 mg/L, and 30 mg/L, respectively.

The commercial non-sintered ceramsite (CNC) was obtained from an environmental protection building materials factory in Zhengzhou City, Henan Province, in China.

2.2 Preparation of foundry dust based non-sintered ceramsite by curing steam

Sodium hydroxide and calcium oxide according to mass ratio of 1:1 were mixed to obtain alkaline activator. Water glass was dissolved in distilled water to obtain 18% of water glass, for use as binder solution. The FD and FA were placed in a drying oven at 105℃ to obtain dried FD and FA. The dried FD was mixed with FA according to mass ratio of 7:3 to obtain the raw material mixture. The raw material was combined with cement and alkaline activator (25% and 10% of mass of raw material respectively) to obtain total mixture. The total mixture was placed in disc pelletizer, which rotated at speed of 42 rpm under a fixed angle of 60°C. After 2 minutes, the disc pelletizer was turned off, and the total mixture was sprayed 30 times with binder solution using a spray bottle to obtain the spherical particle derived from FD with a diameter of 3-8 mm. The spherical particle was cured at room temperature for 2 h, and then transferred to a steam curing pot, and maintained at a temperature of 80˚C for 16 h. Afterwards, the spherical particle was dried to obtain the FD based non-sintered ceramsite produced by the curing steam method (FDNCCS).

ISSN 2616-5880 Vol. 5, Issue 2: 46-54, DOI: 10.25236/AJMC.2024.050208

2.3 Preparation of foundry dust-based non-sintered ceramsite by curing carbon dioxide method

The spherical particle derived from FD was prepared as above. The spherical particle was transferred to a carbonization box for pre-curing for 48 h, with air humidity and temperature were at 70% and 25°C respectively. Afterwards, the pre-curing non-sintered ceramsite was cured in a carbonization box under conditions of 70% air humidity and 20% volume fraction of CO_2 for 2 h to obtain FD based non-sintered ceramsite by CO_2 curing (FDNCCC).

2.4 Design biological aerated filter

A plastic circular tube with internal diameter of 10 cm was used to make biological aerated filters (BAF) (Figure 1), which included a water distribution zone, support layer, filter material layer, and effluent area. The distribution zone with height of 20 cm is positioned below a perforated filter plate included an inlet pipe, backwash air pipe, aeration tube, and discharging sludge pipe. A 6 cm support layer of pebbles with diameter 3-5 cm is positioned above the perforated filter plate, followed by 21 cm biocarrier layer, and a 13cm water storage area. The main structure of BAF is shown in Figure 1.

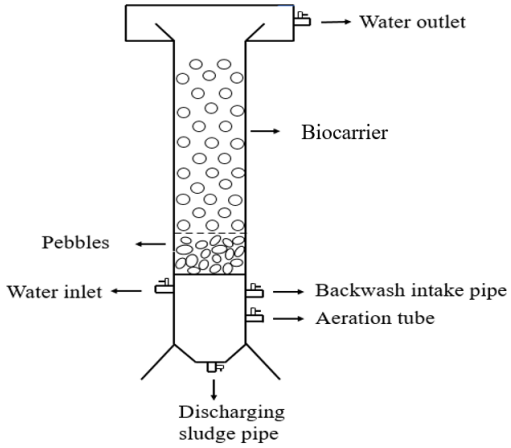

Figure 1: Schematic diagram of experimental device.

2.5 Biofilm formation for BAF filled with CNC and FDNCCC

Activated sludge and wastewater were obtained from a wastewater treatment plant in Jiangbei District, Nanjing City. Activated sludge and wastewater were mixed according to volume ratio of 1:3, and then added into BAF filled with CNC and FDNCCC, respectively. After 3 d, the simulated swine wastewater was pumped into a different BAF according to air-to-water volume ratio of 4:1 and a hydraulic retention time (HRT) of 2 h. Effluent was taken after 3 d, and then analyzed to determine the pH and the concentration of COD, NH_4^+-N, and phosphate. The pollutant removal efficiency was calculated using Equation. (1). The biofilm in the biocarrier was also analysed to determine change in microorganisms present.

$$\eta = \frac{(C_0 - C_1)}{C_0} \times 100\% \quad (1)$$

Where η (%) represents the removal efficiency, C_0 (mg/L) and C_1 (mg/L) represent the influent and effluent concentration, respectively.

2.6 Purifying capacity of swine wastewater by BFA filled with FDNCCC

Swine wastewater was introduced into a BAF filled with FDNCCC, and then operated under the gas-to-water volume ratio of 4:1 and HRT at 2 h. After a period of operation, an effluent sample was taken and analysed for COD, NH_4^+-N, TN, and phosphate content. The removal efficiencies of pollutants were calculated using Equation. (1).

2.7 Analytical methods

The basic performance of CNC, FDNCCS, and FDNCCC, including compressive strength, sum of

ISSN 2616-5880 Vol. 5, Issue 2: 46-54, DOI: 10.25236/AJMC.2024.050208

crushing rate and wear rate, bulk density, density, porosity, and water absorption rate, were determined according to the standard specifications of "Artificial Ceramic Filter Media for Water Treatment" (CJ/T299-2008). The crystal structures and chemical compositions of CNC, FDNCCS, and FDNCCC were analyzed by X-ray diffraction (XRD-6100, Shimadzu Corporation, Japan). Biofilms in BAF were analyzed using an optical microscope with a magnification of 20000 (OM, OLYMPUS CKX53, Japan). Specific surface area, total pore volume and average pore size of CNC, FDNCCS, and FDNCCC were determined using a fully automated gas analyzer (BET, Quantachrome ASiQwin, USA). The concentration of TN was determined by alkaline potassium persulfate digestion ultraviolet spectrophotometry (HJ636-2012). The concentration of COD was determined using the potassium dichromate titration method (HJ828-2017). The concentrations of NH_4^+-N and PO_4^{3-}-P were determined by Nano reagent spectrophotometry (HJ535-2009) and molybdenum antimony spectrophotometry (GB11893-89) using UV–Vis spectrophotometer, respectively.

2.8 Data analysis and processing

The data in this experiment was processed using software Excel 2016, the graphing was done using Origin 2021, and the XRD test results were analyzed using MDI Jade 6.5.

3. Results and Discussion

3.1 Characteristics of foundry dust-based non-sintered ceramsite by CO_2 curing

XRD pattern of CNC indicated that the main material was quartz (Figure. 2 a), and peaks between 20°-30° (2θ) appeared for FDNCCS (Figure 2 b), which are attributed to the amorphous gel phase produced by the gel material, and it could be moganite. As shown in Figure 2 c, XRD pattern of FDNCCC revealed that the main crystal structures are calcite and calcium silicate. Sharma et al. [12] demonstrated that CO_2 could be diffused into the interior of the cement slurry through the pores, and then reacted with calcium ions from $Ca(OH)_2$ to form calcium carbonate. Therefore, calcite produced from FDNCCC could be related to the calcium ions reaction with CO_2 during curing CO_2.

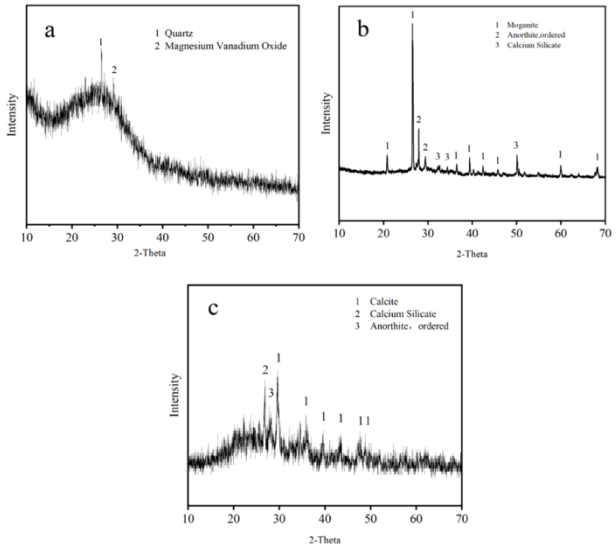

Figure 2: XRD diagrams of CNC (a), FDNCCS (b), and FDNCCC (c).

It can be observed from Figure 2, that the adsorption curves of three ceramsites exhibit a significant increase in N_2 adsorption at the low-pressure end, a slow growth at the medium-pressure end, and a rapid increase at the high-pressure end. The desorption curves exhibit hysteresis phenomena at P/P_0=0.4-1.0 [13]. According to the BDDT classification, the adsorption isotherms of three ceramsites belong to the II type, indicating a strong interaction between the ceramsite and N_2, and that they are non-porous or macroporous adsorption. According to the IUPAC classification, the desorption curves of three ceramsites belong to the H_3 type hysteresis loop, indicating the presence of slit-like pores formed by the accumulation of sheet-like particles. Adsorption saturation is not observed in the higher relative pressure region, indicating irregular pore structure [14]. According to Figure 3, the pore size distribution of the three ceramsites was 3-10 nm, which are mesopores.

ISSN 2616-5880 Vol. 5, Issue 2: 46-54, DOI: 10.25236/AJMC.2024.050208

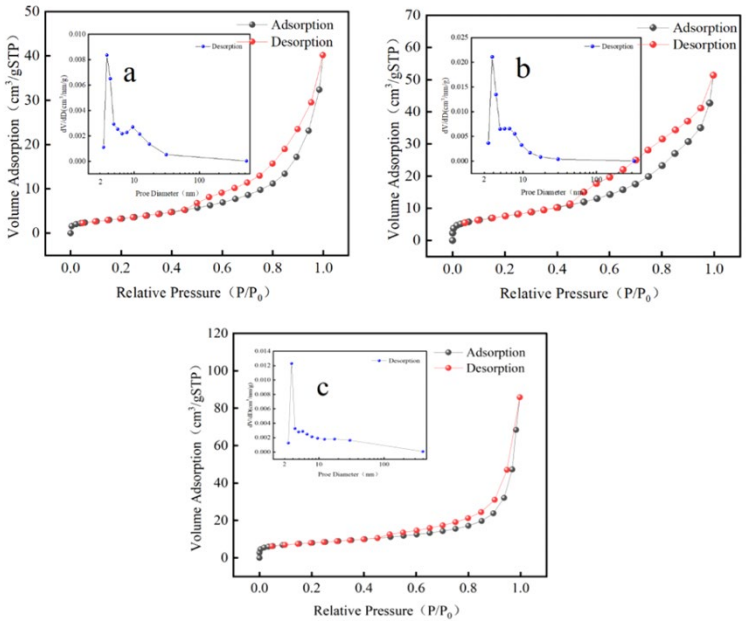

Figure 3: Adsorption and desorption curves and pore size distribution of CNC (a), FDNCCS (b), and FDNCCC (c).

The specific surface areas of CNC, FDNCCS, and FDNCCC are respectively 12.04 m^2/g, 27.46 m^2/g, and 28.11 m^2/g (Table 2), indicating that the specific surface area of the CNC is much smaller than those of non-sintered ceramsite derived from FD. The total pore volumes and the average pore sizes for CNC, FDNCCS, and FDNCCC were 0.0621 cm^3/g and 20.65 nm, 0.0795 cm^3/g and 11.58 nm, and 0.1328 cm^3/g and 18.90 nm, respectively. Results showed that the total pore volume of FDNCCC was nearly twice that of the other two types of ceramsite.

Table 2: Specific surface area, total pore volume, and average pore size of three types of ceramsite.

	Specific surface area (m^2/g)	Total pore volume (cm^3/g)	Average Pore diameter (nm)
FDNCCC	12.04	0.0621	20.65
FDNCCS	27.46	0.0795	11.58
CNC	28.11	0.1328	18.90

Table 3: Basic physical performance indicators of three types of ceramsite.

Test indicators	CNC	FDNCCS	FDNCCC	Standard limits (CJ/T299-2008)
Specific surface area (m^2/g)	12.04	27.46	28.11	$\geq 0.5\times10^4$
Particle size(mm)	3-8	3-8	3-8	-
Sum of crushing rate and wear rate (%)	0.24	0.78	0.67	≤6
Compressive strength (MPa)	16.3	2.34	5.18	-
Bulk density (g/cm^3)	1.08	0.52	0.53	-
Density (g/cm^3)	1.81	0.96	1.02	-
Porosity rate (%)	40.3	45.8	48.1	≥40
Water absorption rate (%)	15.7	27.7	22.4	-

The compressive strengths of FDNCCC, FDNCCS, and CNC are 5.18 MPa, 2.34 MPa, and 16.3 MPa, and the sum of the crushing rate and wear rate, and porosity rate were 0.67% and 48.1%, 0.78% and 45.8%, and 0.24% and 40.3%, respectively meaning that they meet the standards of "Artificial Ceramic Filter Media for Water Treatment" (CJ/T299-2008). As shown in Table 3, compressive strength of FDNCCC (5.18 Mpa) is 2.2 times that of FDNCCS.

3.2 Forming biofilm characteristics of biocarrier of FDNCCC

It can be observed from Figure 4 a, that the COD concentration in the effluent for BAF filled with CNC and FDNCCC at operation day 3 were respectively 813.34 mg/L and 693.33 mg/L, corresponding

ISSN 2616-5880 Vol. 5, Issue 2: 46-54, DOI: 10.25236/AJMC.2024.050208

to their COD removal rates of 35.79% and 45.26%. However, COD concentrations in the effluent from BAF filled CNC and FDNCCC at operation day 10 were 213.33 mg/L and 119.99 mg/L, with removal efficiencies of 82.22% and 90% respectively. Therefore, there is a higher removal rate of COD from the BAF filled with FDNCCC than from the BAF filled with CNC. As shown in Figure 4 b, concentration and removal efficiencies of NH_4^+-N in the effluent from BAF filled with CNC and FDNCCC at operation day 3 were 126.24 mg/L and 21.2%, and 115.07 mg/L and 28.17%, respectively. The lower removal rate of NH_4^+-N before operation day 3 could be related to the lower nitrification efficiency due to nitrifying bacteria with a slower adaptation process and longer generation cycle [15]. The removal rate and concentration of NH_4^+-N in effluent from BAF filled CNC at operation day 10 were 57.01% and 66.29 mg/L compared with 65.45% and 51.31 mg/L for BAF filled with FDNCCC. Therefore, the BAF filled with FDNSCC has a higher removal rate of NH_4^+-N than BAF filled with CNC. Xia et al. [16] demonstrated that biofilm formation on the surface of ceramsite can be regarded as mature when the removal efficiency of COD and NH_4^+-N reach 80.81% and 65.344% after 18 d operation in a column filled with ceramsite derived from dredging sea mud. In this study, the removal efficiency of COD and NH_4^+-N were 90% and 65.45% for BAF filled with FDNCCC at operation day 10, indicating that the biofilm matured much quicker when using foundry dust based non-sintered ceramsite formed by curing CO_2.

The removal efficiency of phosphate for BAF filled with FDNCCC was higher than that of BAF filled with CNC (Figure 4 c). For example, removal efficiencies of phosphates from BAF filled with CNC and FDNCCC at operation day 10 were 60.83% and 77.41% respectively. The higher removal efficiency of phosphate from BAF filled with FDNCCC was associated with the rapid growth of the biofilm [17]. In addition, a large amount of calcium from ceramsite could react with phosphates to form precipitates, resulting in enhancing the removal efficiency of phosphate.

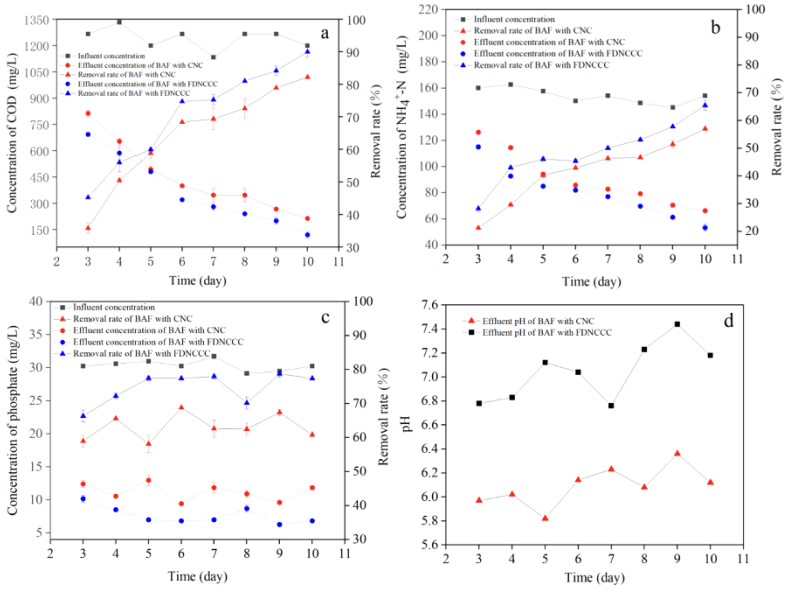

Figure 4 : The removal rate COD (a), NH_4^+- N (b), phosphate (c) and pH (d) from BAF filled with CNSC and FDNSCC.

It can be observed from Figure 4 d, that effluent pH from BAF filled with CNC ranged from 5.82 to 6.36 compared with 6.76 to 7.44 from BAF filled with FDNCCC. Microorganism growth will be hindered when the pH is acidic. Similarly, the equilibrium state of the cell membrane will be disrupted when alkalinity is too strong, resulting in a negative impact on microbial growth[18]. Compared to CNC, pH in BAF filled with FDNCCC is more suitable for microbial growth, resulting in the higher removal rates of COD, NH_4^+- N and phosphate (Figure 4 a, b, c).

A few ciliates and nematodes occur in BAF filled with CNC at operation 7 d (Figure 3.4a, b), whereas many metazoan[19], such as rotifers, ciliates, nematodes, and suctoria, appeared in BAF filled with FDNCCC (Figure 5 c, d, e, f). The type of metazoan could be used to judge the maturity status of biofilms[20] Results showed that the biofilm maturation on the surface of biocarrier of FDNCC occurs after operation 7 d, Xia et al.[16] reported that biofilm maturation on the surface of biocarrier of ceramsite derived from dredging sea mud needed 18 d. These findings indicate that the biofilm could be more easily formed on the surface of FDNCC because it has a larger specific surface area supporting microbial

ISSN 2616-5880 Vol. 5, Issue 2: 46-54, DOI: 10.25236/AJMC.2024.050208

attachment and organism growth [21].

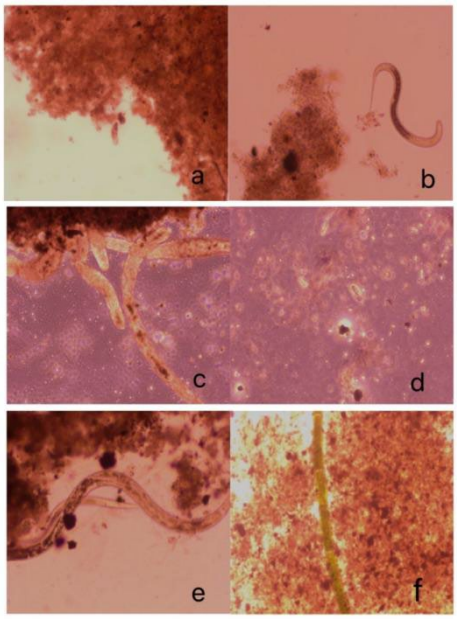

Figure 5: Optical electron microscopy examination of biofilm from BAF filled with CNC (a,b) and FDNCCC (c, d, e, f).

3.3 Purification capacity of swine wastewater by BAF filled with FDNCCC

It can be observed from Figure 6 a, that the concentration of COD in effluent from BAF was below 100 mg/L when the influent COD concentration of swine wastewater ranged from 373.33 to 506.67 mg/L, and a removal rate of 75% - 85% was achieved in BAF filled with FDNCCC. These results are similar to those of Wu et al.[22] who found that the removal rate of COD was between 69.91% and 87.77% for spong iron and ceramsite mixed fillers as biocarrier when the influent COD concentration was 232.9 mg/L. According to Figure 6 b, NH_4^+-N concentration in effluent is below 20 mg/L when NH_4^+-N concentration in influent of swine wastewater is between 88.09 -112.59 mg/L, indicating that a removal rate between 80% - 90% was obtained for BAF filled with FDNCCC. Chai et al.[23] found that the NH_4^+-N removal rate of 47.33% was achieved for BAF filled with sintered ceramsite derived from tailings and blast furnace slag. These finding showed that a higher removal rate of NH_4^+-N was obtained for BAF with FDNCCC as biocarrier than sintered ceramsite as biocarrier.

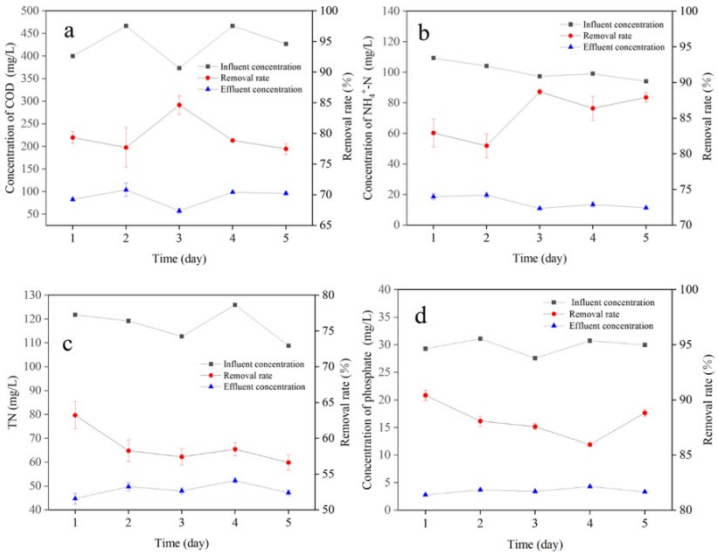

Figure 6: Concentration and removal rate of COD (a), NH_4^+-N (b), TN (c), and phosphate from BAF filled with FDNCCC.

ISSN 2616-5880 Vol. 5, Issue 2: 46-54, DOI: 10.25236/AJMC.2024.050208

The TN concentration in effluent from BAF filled with FDNCCC was below 50 mg/L when TN concentration of swine wastewater in influent was between 106.73 - 131.23 mg/L, indicating that a removal rate of TN between 55% - 65% (Figure 6 c) was achieved. This was higher than the removal rate of TN of 50% achieved by sintered ceramsite derived from sludge and coal fly ash[24]. In this study, the removal rate of phosphate was 85% for BAF filled with FDNCCC when the phosphate concentration of effluent was below 5 mg/L under phosphate concentration in influent from swine wastewater is 27.19 - 32.22 mg/L (Figure 6 d). As shown in Figure 6, the concentration in effluent from BAF of pollutants such as COD, NH_4^+-N, and phosphate, was lower than the discharge standard of 400 mg/L COD, 80 mg/L NH_4^+-N, and 5 mg/L phosphate as stipulated by Discharge Standard of Pollutants for Livestock and Poultry Breeding of China (GB18596-2001). These findings indicate that the BAF filled with FD-based non-sintered ceramsite curing by CO_2 can be applied to treatment swine wastewater.

4. Conclusion

(1) CO_2 curing method was successfully used to prepare the non-sintered ceramsite derived from FD. The FD-based non-sintered ceramsite (FDNCCC) was obtained under air humidity at 70%, temperature at 20°C, and CO_2 volume fraction of 20%.

(2) The compressive strength, sum of the crushing rate and wear rate, specific surface area, and water absorption rate were respectively 5.18 MPa, 0.67%, 48.1%, and 22.4% for FDNCCC. These met the standards of "Artificial Ceramic Filter Media for Water Treatment" (CJ/T299-2008). Compressive strengths of FDNCCC are 2.2 times than that FDNCCS obtained by curing steam.

(3) It is easier to form biofilm for FDNCCC as biocarrier than commercial non-sintered ceramsite (CNC). The removal rate of COD, NH_4^+-N, TN, and phosphate was respectively 75% - 85%, 80% - 90%, 55% - 65%, and >85% were obtained for BAF filled with FDNCCC under HRT at 2 h, and gas-to-water ratio at 4:1. Their concentration in effluent was lower than those stipulated by the Discharge Standard of Pollutants for Livestock and Poultry Breeding of China (GB18596-2001). It is found that FDNCCC can be applied to treat swine wastewater effectively and efficiently.

References

[1] Chen X, Lin H, Dong Y, Li B, Yin T, Liu C. Simultaneous high-efficiency removal of sulfamethoxazole and zinc (II) from livestock and poultry breeding wastewater by a novel dual-functional bacterium, Bacillus sp. SDB4 [J]. Environmental Science and Pollution Research, 2022, 29(4): 6237-6250.
[2] Giannuzzi L, Sedan D, Echenique R, Andrinolo D. An acute case of intoxication with cyanobacteria and cyanotoxins in recreational water in Salto Grande Dam, Argentina [J]. Maring Drugs, 2011, 9(11): 2164-2175.
[3] Wang S, Zhang Z, Wang N, et al. FLUENT simulation design and optimization of biological aerated filter [J]. Journal of Physics: Conference Series, 2022, 2148(1).
[4] Wan Q, Song H, Ju K, et al. Purification of eutrophic river water using a biological aerated filter with functional filler [J]. Polish Journal of Environmental Studies, 2021, 30(2): 1841-1852.
[5] Yu T, Linshi J, Miao Y, et al. Study on treatment of domestic wastewater by biological aerated filter [J]. IOP Conference Series: Earth and Environmental Science, 2019, 330(3).
[6] Liu D, Wang X, Li X, et al. Study of ammonia removal efficiency and process regulation strategy of biological aerated filter in treating low-temperature micropolluted urban landscape water [J]. Journal of Environmental Engineering, 2023, 149(4).
[7] Xin X, Liu S, Qin J, et al. Performances of simultaneous enhanced removal of nitrogen and phosphorus via biological aerated filter with biochar as fillers under low dissolved oxygen for digested swine wastewater treatment [J]. Bioprocess and Biosystems Engineering, 2021, 44(8): 1741-1753.
[8] Xu F, Liu W, Bu S, et al. Manufacturing non-sintered ceramsite from incinerated municipal solid waste ash (IMSWA): Production and performance [J]. Process Safety and Environmental Protection, 2022, 163: 116-130.
[9] Shi Y, Guo W, Jia Y, et al. Preparation of non-sintered lightweight aggregate ceramsite based on red mud-carbide slag-fly ash: Strength and curing method optimization [J]. Journal of Cleaner Production, 2022, 372.
[10] Zhu J, Qu Z, Liang S, et al. Macroscopic and microscopic properties of cement paste with carbon dioxide curing [J]. Materials (Basel), 2022, 15(4).
[11] Harirchi P, Yang M. Exploration of carbon dioxide curing of low reactive alkali-activated fly ash [J]. Materials (Basel), 2022, 15(9).

ISSN 2616-5880 Vol. 5, Issue 2: 46-54, DOI: 10.25236/AJMC.2024.050208

[12] Sharma R, Kim H, Pei J, et al. Dimensional stability of belite-rich cement subject to early carbonation curing [J]. Journal of Building Engineering, 2023, 63.
[13] Zhang Y, Yang M, Gui H, et al. Study on the denitrification and dephosphorization of the aqueous solution by Chitosan/4A Zeolite/Zr based Zeolite [J]. Environmental Technology, 2021, 42(2): 227-237.
[14] Dong X Y M, Li Y Y, Li S H, et al. Insight into the CO2 capturer derived from graphene/MgO composite [J]. Clean - Soil Air Water, 2017, 45(7).
[15] Wang L, Zhu N, Shaghaleh H, et al. The effect of functional ceramsite in a moving bed biofilm reactor and its ammonium nitrogen adsorption mechanism [J]. Water, 2023, 15(7).
[16] Xia T, Li Y, Xiao Z, et al. A Study on ceramsite production using dredging sea mud and its biofilm formation capacity evaluation [J]. Advances in Civil Engineering, 2018, 2018: 1-9.
[17] Wang Y K, Pan X R, Geng Y K, et al. Simultaneous effective carbon and nitrogen removals and phosphorus recovery in an intermittently aerated membrane bioreactor integrated system [J]. Scientific Reports, 2015, 5: 16281.
[18] Chen S, Chen Y, Pei H, et al. Biofilm development dynamics and pollutant removal performance of ceramsite made from drinking-water treatment sludge [J]. Water Environmental Research, 2019, 91(7): 616-627.
[19] Feng L, He Q, Wen J. A bioaugmentation agent allowing the advanced treatment of refractory refinery wastewater in a biological aerated filter and analysis of its microbial community [J]. Journal of Chemical Technology & Biotechnology, 2020, 95(4): 1258-1269.
[20] Nikoonahad A, Ghaneian M T, Mahvi A H, et al. Application of novel modified biological serated filter (MBAF) as a promising post-treatment for water reuse: modification in configuration and backwashing process [J]. Journal of Environmental Management, 2017, 203(Pt 1): 191-199.
[21] Bao T, Chen T, Liu H, et al. Preparation of magnetic porous ceramsite and its application in biological aerated filters [J]. Journal of Water Process Engineering, 2014, 4: 185-195.
[22] Wu Y, Dai J, Wan Q, Tian G, Wei D, Vignali V. Purification of Urban Sewage River Using a Biological Aerated Filter with Sponge Iron and Ceramsite Mixed Fillers [J]. Advances in Civil Engineering*, 2020, 1-10.*
[23] Chai Y, Hu W, Zhang Y, et al. Process and property optimization of ceramsite preparation by Bayan Obo tailings and blast furnace slag [J]. Journal of Iron and Steel Research International, 2023, 30(7): 1381-1389.
[24] Wan Q, Han Q, Luo H, et al. Ceramsite facilitated microbial degradation of pollutants in domestic wastewater [J]. International Journal of Environmental Research and Public Health, 2020, 17(13).